


# Positive magnetoresistance of single-crystal bilayer manganites $(\text{La}_{1-z}\text{Nd}_z)_{1.4}\text{Sr}_{1.6}\text{Mn}_2\text{O}_7$ ( $z = 0, 0.1$ )

Cite as: J. Appl. Phys. **117**, 163918 (2015); <https://doi.org/10.1063/1.4918916>

Submitted: 01 February 2015 . Accepted: 13 April 2015 . Published Online: 29 April 2015

K. A. Shaykhtudinov, S. E. Nikitin, M. I. Petrov, K. I. Terent'ev, S. V. Semenov, and S. I. Popkov 



View Online



Export Citation



CrossMark

## ARTICLES YOU MAY BE INTERESTED IN

Magnetoresistance of substituted lanthanum manganites  $\text{La}_{0.7}\text{Ca}_{0.3}\text{MnO}_3$  upon nonequilibrium overheating of carriers

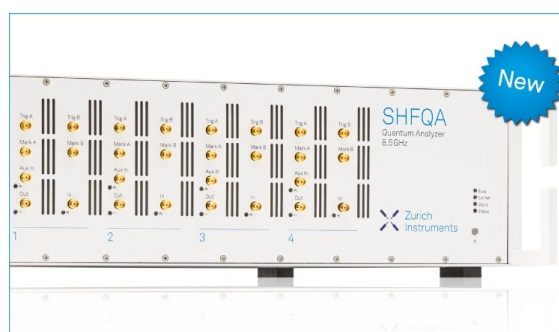
Journal of Applied Physics **109**, 083711 (2011); <https://doi.org/10.1063/1.3573666>

Magnetic-field- and bias-sensitive conductivity of a hybrid  $\text{Fe}/\text{SiO}_2/\text{p-Si}$  structure in planar geometry

Journal of Applied Physics **109**, 123924 (2011); <https://doi.org/10.1063/1.3600056>

CAMEA—A novel multiplexing analyzer for neutron spectroscopy

Review of Scientific Instruments **87**, 035109 (2016); <https://doi.org/10.1063/1.4943208>



## Your Qubits. Measured.

Meet the next generation of quantum analyzers

- Readout for up to 64 qubits
- Operation at up to 8.5 GHz, mixer-calibration-free
- Signal optimization with minimal latency

Find out more



## Positive magnetoresistance of single-crystal bilayer manganites ( $\text{La}_{1-z}\text{Nd}_z$ ) $_{1.4}\text{Sr}_{1.6}\text{Mn}_2\text{O}_7$ ( $z = 0, 0.1$ )

K. A. Shaykhutdinov,<sup>1</sup> S. E. Nikitin,<sup>1,2</sup> M. I. Petrov,<sup>1</sup> K. I. Terent'ev,<sup>1</sup> S. V. Semenov,<sup>1</sup>  
and S. I. Popkov<sup>1</sup>

<sup>1</sup>*Kirensky Institute of Physics, Akademgorodok 50, bld. 38, Krasnoyarsk 660036, Russia*

<sup>2</sup>*Siberian Federal University, pr. Svobodny 79, Krasnoyarsk 660041, Russia*

(Received 1 February 2015; accepted 13 April 2015; published online 29 April 2015)

We investigate magnetoresistance,  $\rho_c$ , of single-crystal bilayer lanthanum manganites ( $\text{La}_{1-z}\text{Nd}_z$ ) $_{1.4}\text{Sr}_{1.6}\text{Mn}_2\text{O}_7$  ( $z = 0$  and  $0.1$ ) at a transport current flowing along the crystal  $c$  axis and in external magnetic fields applied parallel to the crystal  $c$  axis or  $ab$  plane. It is demonstrated that the  $\text{La}_{1.4}\text{Sr}_{1.6}\text{Mn}_2\text{O}_7$  manganite exhibits the positive magnetoresistance effect in the magnetic field applied in the  $ab$  sample plane at the temperatures  $T < 60$  K, along with the negative magnetoresistance typical of all the substituted lanthanum manganites. In the ( $\text{La}_{0.9}\text{Nd}_{0.1}$ ) $_{1.4}\text{Sr}_{1.6}\text{Mn}_2\text{O}_7$  sample, the positive magnetoresistance effect is observed at temperatures of 60–80 K in an applied field parallel to the  $c$  axis. The mechanism of this effect is shown to be fundamentally different from the colossal magnetoresistance effect typical of lanthanum manganites. The positive magnetoresistance originates from spin-dependent tunneling of carriers between the manganese-oxygen bilayers and can be explained by features of the magnetic structure of the investigated compounds. © 2015 AIP Publishing LLC. [<http://dx.doi.org/10.1063/1.4918916>]

### INTRODUCTION

The discovery of colossal magnetoresistance (CMR) in manganites stimulated a great interest in these materials from fundamental and practical points of view.<sup>1,2</sup> For a few years, the CMR reading heads have been used in magnetic storage industry.<sup>2</sup> Manganites are characterized by a rich phase diagram involving the charge and orbital ordering regions.<sup>1,2</sup> Study of the interaction between the orbital and spin degrees of freedom in these compounds is of great importance. The metal-insulator transition found in manganites and the related CMR effect is usually described using the double exchange mechanism proposed by Zener,<sup>3</sup> which includes the local exchange coupling between conduction electrons  $e_g$  and localized electrons  $t_{2g}$  that form the atomic spin  $S = 3/2$ . However, as was shown in some studies,<sup>4</sup> the correct description of the physical phenomena in manganites should take into account the electron-lattice interaction.

Bilayer lanthanum manganites belong to the Ruddlesden-Popper series ( $\text{R}_{2-2x}\text{A}_{1+x}$ ) $_{n+1}\text{Mn}_n\text{O}_{3n+1}$  with  $n = 2$ .<sup>5,6</sup> The crystals of this composition (I4/mmm sp. gr.) consist of  $\text{MnO}_2$  layers separated by rock salt layers and  $\text{MnO}_6$  octahedra that form a 2D network. These compounds undergo the metal-insulator transition, at which a high magnetoresistance is observed. The initial  $\text{La}_3\text{Mn}_2\text{O}_7$  compound is an antiferromagnetic insulator (AFI); however, replacing of  $\text{La}^{3+}$  by cations of different valence can change the electronic structure of manganese ions  $\text{Mn}^{3+}$  and lengths and angles of the Mn-O bonds.<sup>7,8</sup> Non-isovalent substitution of  $\text{Sr}^{2+}$  for  $\text{La}^{3+}$  changes the manganese oxidation degree from  $\text{Mn}^{3+}$  to  $\text{Mn}^{4+}$ ; as a result, the hole conductivity arises and the mixed-valence state is established between  $\text{Mn}^{3+}$  and  $\text{Mn}^{4+}$  ions with the respective  $3d^4$  and  $3d^3$  electronic configurations. The  $x$  value in the  $\text{La}_{2-2x}\text{Sr}_{1+2x}\text{Mn}_2\text{O}_7$  compound indicates the fraction

of  $\text{Mn}^{4+}$  ions in the entire Mn content and corresponds to the number of holes in the  $\text{Mn}^{4+}/\text{Mn}^{3+}$  pairs.<sup>9</sup>

In studies,<sup>10,11</sup> the strong change in the magnetotransport properties of the ( $\text{La}_{1-z}\text{Nd}_z$ ) $_{2-2x}\text{Sr}_{1+2x}\text{Mn}_2\text{O}_7$  compound were observed upon substitution of  $\text{Nd}^{3+}$  ions with the smaller ionic radius for  $\text{La}^{3+}$  ions, which was attributed to complexity of the magnetic structure of the system. Neutron diffraction data showed that in the compounds with  $x = 0.4$  and  $0.5$  ( $z = 0$ ) the easy axis lies in the  $ab$  plane and the ground states are ferromagnetic and antiferromagnetic, respectively, in contrast to the weakly ferromagnetically ordered composition with  $x = 0.3$ , in which the easy axis is perpendicular to the  $ab$  plane.<sup>9,10,12,13</sup> The magnetotransport properties of such systems were studied by many authors;<sup>1,9,14–16</sup> however, the magnetoresistance anisotropy in the region of small  $x$  has been understudied. So, in this report, we investigate the compositions with  $x = 0.3$ , in view of the following. As is known, at the concentrations  $0.3 = \langle x \rangle < 0.32$ , the AFM interlayer exchange is sharply changed for the FM one and at  $x > 0.45$  the canted A-type AFM ordering already prevails with the  $dx^2 - y^2$  orbital involved.<sup>1,17</sup> Thus, at this concentration of carriers near the critical point, the spin-reorientation transitions and some related phenomena in bilayer manganites can be easily induced with the help of external factors, including temperature, magnetic field, hydrostatic, and chemical pressure.<sup>18,19</sup>

Substitution of  $\text{Nd}^{+3}$  or  $\text{Pr}^{+3}$  ions with a smaller radius for  $\text{La}^{+3}$  ions significantly affects the magnetotransport characteristics of bilayer manganites.<sup>11,12,17</sup> The neutron diffraction data reported in a study<sup>12</sup> are indicative of the strong variation in lattice parameters  $a$  and  $c$ . This effect of chemical pressure leads to the enhanced Jahn–Teller steady-state distortion and the observed change in the orbital character of  $e_g$  electrons from  $d3z^2 - r^2$  to  $dx^2 - y^2$ .<sup>12</sup>

The  $\text{La}_{1.4}\text{Sr}_{1.6}\text{Mn}_2\text{O}_7$  crystal undergoes the paramagnetic insulator-canted ferromagnetic metal transition at the temperature  $T_c = 110$  K, which is accompanied by the linear lattice contraction along the  $c$  axis.<sup>10</sup> The bilayer manganites are characterized by the strong anisotropy of physical properties in different crystallographic directions. The  $\text{La}_{1.4}\text{Sr}_{1.6}\text{Mn}_2\text{O}_7$  crystal has the easy magnetization axis parallel to the crystal  $c$  axis; the electrical resistivity of this material along the  $c$  axis exceeds that in the  $ab$  plane by several orders of magnitude.<sup>1</sup>

In this work, we investigate the magnetotransport properties of the  $(\text{La}_{1-z}\text{Nd}_z)_{2-2x}\text{Sr}_{1+2x}\text{Mn}_2\text{O}_7$  ( $x = 0.3$  and  $z = 0$  and  $0.1$ ) compounds in external magnetic fields applied parallel and perpendicular to the crystal  $c$  axis.

## EXPERIMENTAL

Single-crystal  $(\text{La}_{1-z}\text{Nd}_z)_{1.4}\text{Sr}_{1.6}\text{Mn}_2\text{O}_7$  ( $z = 0$  and  $0.1$ ) compounds were synthesized using an optical floating zone technique in oxygen atmosphere at a growth rate of 5 mm/h and relative rods rotation speed of 30 rpm.

The magnetotransport and magnetic properties were measured on a commercial Physical Property Measurement System PPMS-9 (Quantum Design) and a vibrating sample magnetometer with a superconducting solenoid.<sup>20</sup> Samples for measurements were cleaved from the synthesized single-crystal rod.

The X-ray diffraction analysis of the powders prepared from the initial single crystals showed that the both samples belong to the  $I4/mmm$  space group with the lattice parameters  $a = 3.858$  Å and  $c = 20.304$  Å for  $\text{La}_{1.4}\text{Sr}_{1.6}\text{Mn}_2\text{O}_7$  and  $a = 3.857$  Å and  $c = 20.317$  Å for  $(\text{La}_{0.9}\text{Nd}_{0.1})_{1.4}\text{Sr}_{1.6}\text{Mn}_2\text{O}_7$ , which are consistent with the data reported in Ref. 21.

The true ratio between neodymium and lanthanum was determined on the natural cleavage plane of the samples by the X-ray fluorescent analysis with the use of a scanning electron microscope and was found to be 9:1 with a relative error of 1%.

Resistivity  $\rho_c$  along the crystal  $c$  axis was measured using a four-probe technique. Two contacts were formed on each flat plane perpendicular to the  $c$  axis. Transport measurements were performed on the samples  $4 \times 2.5 \times 0.3$  mm in size. The contacts were fixed using an Epo-tek H20E two-component adhesive. In the resistivity measurements, the applied magnetic field was parallel to the  $ab$  plane ( $H \parallel ab$ ) or the  $c$  axis ( $H \parallel c$ ) of the crystal.

## RESULTS AND DISCUSSION

Figure 1 shows the experimental temperature dependence of resistivity  $\rho_c(T)$  for the initial  $\text{La}_{1.4}\text{Sr}_{1.6}\text{Mn}_2\text{O}_7$  ( $x = 0.3$  and  $z = 0$ ) compound. It can be seen that at the temperature  $T_c = 110$  K the sample undergoes the metal-insulator transition typical of manganites, which is accompanied by FM ordering of the bilayers.<sup>13</sup> In zero magnetic field, there is a local maximum in the  $\rho_c(T)$  curve at the temperature  $T_{c2} = 65$  K, which coincides with the temperatures of the maximum in the  $M_c(T)$  curve at  $H = 100$  Oe (Fig. 2) and the minimum in the  $M_{ab}(T)$  curve at  $H = 100$  Oe and corresponds to the occurrence of the canted AFM ordering in a

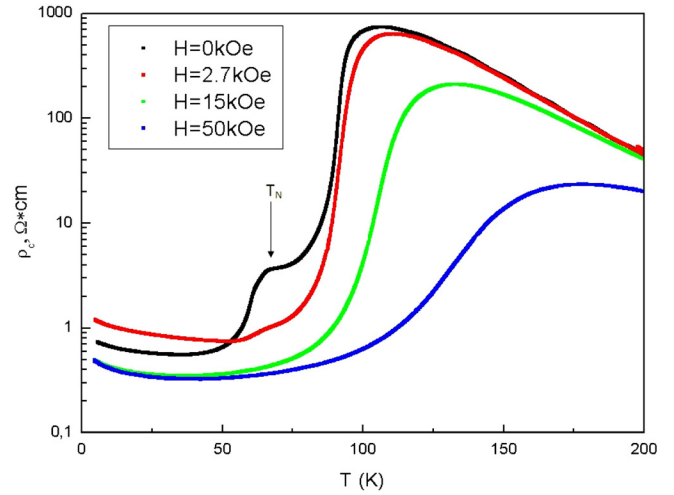


FIG. 1. Temperature dependence of out-of-plane resistivity  $\rho_c$  for the  $\text{La}_{1.4}\text{Sr}_{1.6}\text{Mn}_2\text{O}_7$  single crystal in different magnetic fields  $H$ , applied along the  $c$  axis.

part of the sample.<sup>13</sup> The similar sensitivity of resistivity to Neel temperature were reported for the  $\text{RBa}_2\text{Cu}_3\text{O}_{6+x}$  ( $R = \text{Lu}, \text{Y}$ ) superconductors in the study.<sup>22</sup>

The additional maximum is suppressed by an external magnetic field. In a field of 15 kOe, the maximum disappears. At temperatures  $T < T_c$ , the resistivity of the sample in the field  $H = 2$  kOe ( $H \parallel ab$ ) exceeds the value measured in zero field. As the magnetic field is increased, the resistivity decreases. To thoroughly investigate this feature, we measured the  $\rho_c(H)$  dependences in the temperature range  $T = 2-80$  K. Figure 3 shows that the sample resistivity increases in fields up to the critical field  $H_c \sim 3$  kOe; then the effect changes its sign and, after that we observe the negative magnetoresistance effect typical of manganites until the resistivity saturation at  $H = 20$  kOe.

In our previous work,<sup>23</sup> the effect of positive magnetoresistance was observed in perovskite manganites, but the reason of the effect was quite different. If the Current-Voltage Characteristics (CVCs) of the substituted lanthanum

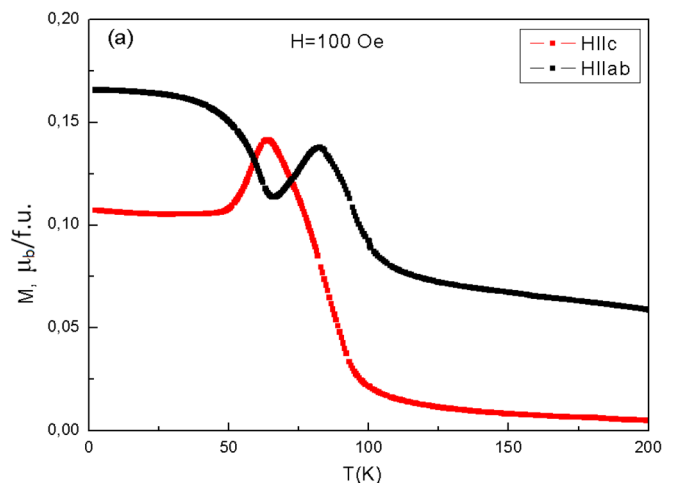


FIG. 2. Temperature dependence of in-plane magnetization  $M_{ab}$  and out-of-plane magnetization  $M_c$  for the  $\text{La}_{1.4}\text{Sr}_{1.6}\text{Mn}_2\text{O}_7$  single crystal in a magnetic field of 100 Oe.

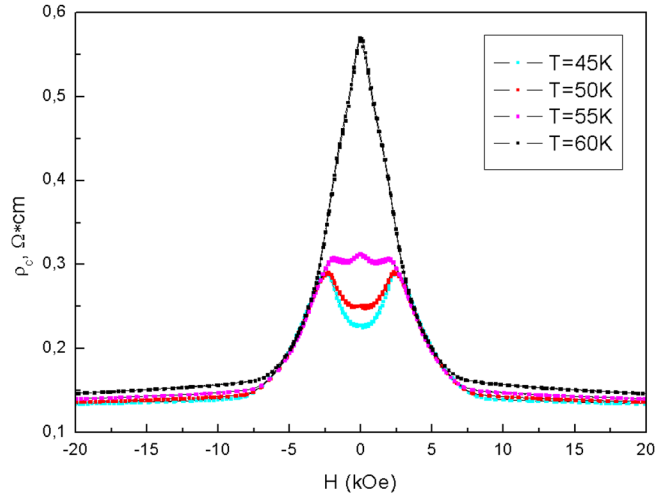


FIG. 3. Magnetic-field dependence of out-of-plane resistivity  $\rho_c$  of the  $\text{La}_{1.4}\text{Sr}_{1.6}\text{Mn}_2\text{O}_7$  single crystal at different temperatures in the field applied along the  $ab$  plane.

manganites are determined by the nonequilibrium overheating of carriers, they become strongly non-linear. As a consequence, the  $\rho(H)$  dependences become extremely sensitive to the value of measuring current  $j$  and sometimes have portions of positive magnetoresistance. In case of the  $(\text{La}_{1-z}\text{Nd}_z)_{1.4}\text{Sr}_{1.6}\text{Mn}_2\text{O}_7$  samples, the value of transport current was extremely small ( $j=0.1 \text{ A/cm}^2$ ) and CVCs were always linear and we never observed the overheating of the samples during measurements.

It can be seen that the resistivity and magnetization of the sample saturate in the same applied magnetic field (see Figs. 4 and 5). It should be noted that the positive magnetoresistance effect is not observed in magnetic fields applied along the  $c$  axis (Fig. 4).

The positive magnetoresistance effect was also observed in the  $(\text{La}_{0.9}\text{Nd}_{0.1})_{1.4}\text{Sr}_{1.6}\text{Mn}_2\text{O}_7$  sample, but at different temperatures and fields than in the initial  $\text{La}_{1.4}\text{Sr}_{1.6}\text{Mn}_2\text{O}_7$  compound. Figure 6 shows temperature dependencies of resistivity obtained in different magnetic fields applied along

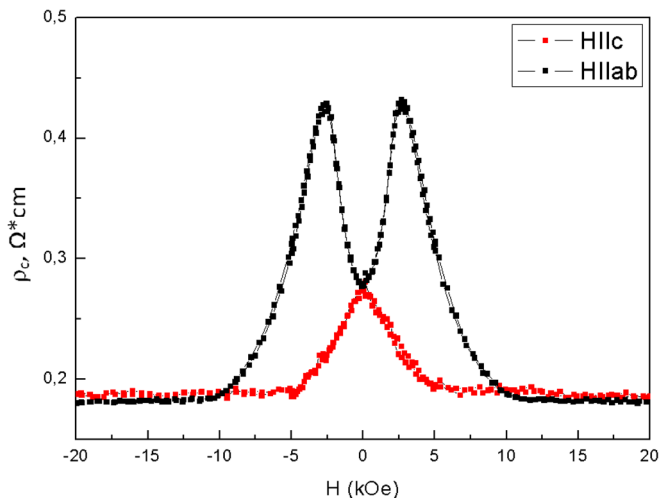


FIG. 4. Magnetic-field dependence of out-of-plane resistivity  $\rho_c$  for the  $\text{La}_{1.4}\text{Sr}_{1.6}\text{Mn}_2\text{O}_7$  single crystal at  $T=4.2 \text{ K}$  in the field applied along the  $c$  axis and in the  $ab$  plane.

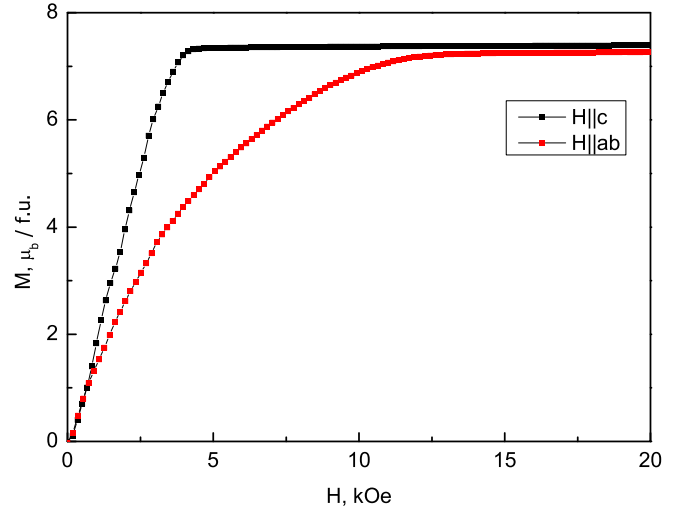


FIG. 5. In-plane magnetization  $M_{ab}$  and out-of-plane magnetization  $M_c$  for the  $\text{La}_{1.4}\text{Sr}_{1.6}\text{Mn}_2\text{O}_7$  single crystal at  $T=4.2 \text{ K}$ .

the  $c$  axis. Analogously to the initial compound, with a decrease in temperature to  $T_c=90 \text{ K}$  the sample undergoes the metal-insulator transition accompanied by the resistivity drop. With a further decrease in temperature, the anomaly is observed in the  $\rho_c(T)$  dependence at  $T_{c2}=60 \text{ K}$  in zero magnetic field. This anomaly contributes to the resistivity. The temperature of the anomaly coincides with the temperature of AFM ordering of the sample (see Fig. 7). When the magnetic field is applied, the anomaly is gradually smoothed and completely vanishes at  $H=15 \text{ kOe}$ . After that, the behavior of the  $\rho_c(T)$  curve with decreasing temperature is similar to that for the initial compound. The feature observed at  $T=65 \text{ K}$  is related to the occurrence of the positive magnetoresistance (Fig. 6). To investigate the positive magnetoresistance effect, we measured the  $\rho_c(H)$  dependences in the temperature region  $60\text{--}80 \text{ K}$  (see Fig. 8). It can be seen that in external magnetic fields of up to  $H_c \sim 3 \text{ kOe}$ , the negative magnetoresistance effect is observed in the sample. Above critical field  $H_c$ , the effect changes its sign and the positive

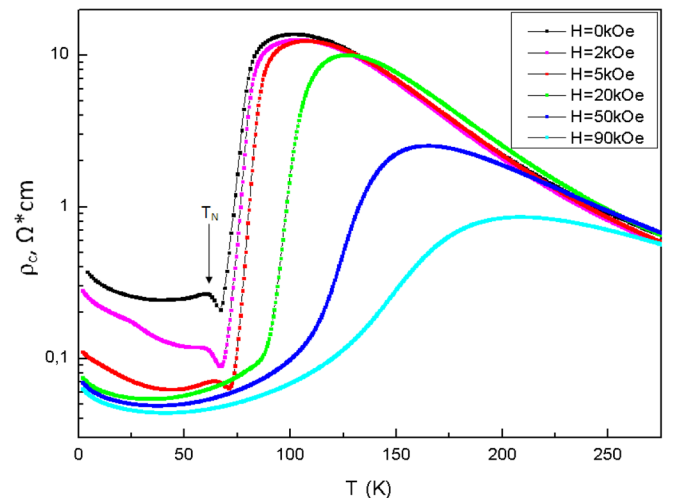


FIG. 6. Temperature dependence of out-of-plane resistivity  $\rho_c$  for the  $(\text{La}_{0.9}\text{Nd}_{0.1})_{1.4}\text{Sr}_{1.6}\text{Mn}_2\text{O}_7$  single crystal in different magnetic fields  $H$  applied along the  $c$  axis.

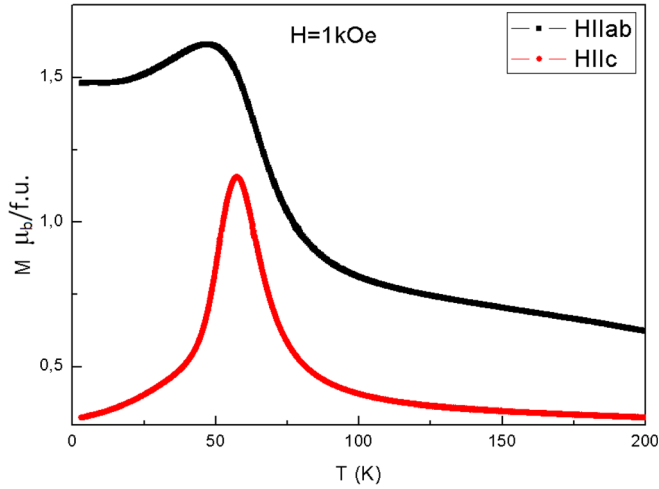


FIG. 7. Temperature dependence of in-plane magnetization  $M_{ab}$  and out-of-plane magnetization  $M_c$  in a magnetic field of 1 kOe for the  $(\text{La}_{0.9}\text{Nd}_{0.1})_{1.4}\text{Sr}_{1.6}\text{Mn}_2\text{O}_7$  single crystal.

magnetoresistance effect is observed in fields of 3–10 kOe. In the field  $H_{c2} \sim 10$  kOe, the effect changes its sign again and with a further increase in the magnetic field the resistance slightly decreases. The effect is observed in the temperature range of  $70 \text{ K} < T < 80 \text{ K}$ .

We start the discussion of the observed effect with the consideration of the magnetic structure of the initial  $\text{La}_{1.4}\text{Sr}_{1.6}\text{Mn}_2\text{O}_7$  compound at temperatures  $T < T_{c2}$ . According to the results reported in Ref. 13, in the initial compound the bonds in the bilayers are always ferromagnetic in the  $ab$  plane, while the magnetic ordering between the bilayers can be both AFM and canted FM along the  $c$  axis. In general, the state with the coexisting AFM and canted FM phases is implemented (See Fig. 9).

Let us consider the magnetization of the initial compound in a magnetic field applied along the  $c$  axis ( $H \parallel c$ ) at  $T < T_{c2}$  (Fig. 4). In this case, canted spins of manganese ions in the FM phase rotate (the initial angle is  $\theta \sim 10^\circ$  (Ref. 13))

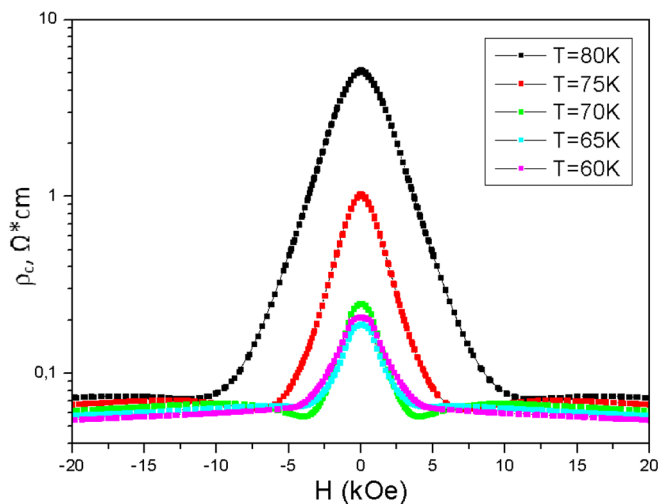


FIG. 8. Magnetic-field dependence of out-of-plane resistivity  $\rho_c$  for the  $(\text{La}_{0.9}\text{Nd}_{0.1})_{1.4}\text{Sr}_{1.6}\text{Mn}_2\text{O}_7$  single crystal at different temperatures in the field applied along the  $c$  axis.

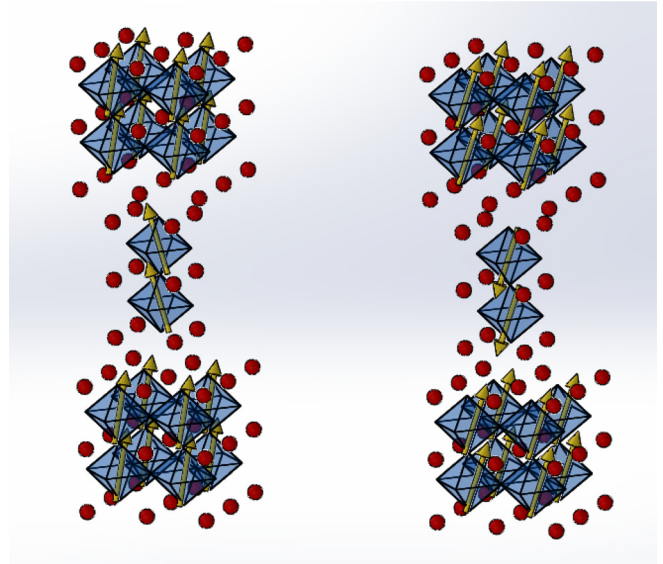


FIG. 9. Schematic view of magnetic structure  $\text{La}_{1.4}\text{Sr}_{1.6}\text{Mn}_2\text{O}_7$  according to the work.<sup>13</sup>

and the magnetic moments of the AFM phase, which lie in the  $ab$  plane, are aligned along the field direction. This results in the drop of resistivity  $\rho_c$  because, according to the double-exchange mechanism, the translation integral is  $t \sim \cos(\theta/2)$ ,<sup>24</sup> where  $\theta$  is the angle between spins of manganese ions. In a magnetic field of 5 kOe, in which all the spins are aligned along the  $c$  axis, the magnetization attains its maximum value  $M_{\text{sat}} = 7.8 \mu_B/\text{f.u.}$  (Fig. 5) and the resistivity reaches its minimum value and stays unchanged as the magnetic field is further increased.

In the magnetic field applied in the  $ab$  plane, the magnetization process is essentially different. In magnetic fields of up to 3 kOe, the magnetic moments of the FM bilayers lie in the  $ab$  plane, which is accompanied by the resistivity growth, since the angle between spins of  $\text{Mn}^{3+}$  and  $\text{Mn}^{4+}$  ions increases due to the AFM exchange between the bilayers.<sup>13</sup> When the magnetic field exceeds the value  $H_c = 3$  kOe, all the magnetic moments of the FM bilayers are ordered in the  $ab$  plane. With a further increase in the magnetic field, the spins in the  $ab$  plane are completely aligned along the magnetic field direction. The angle between the spins of  $\text{Mn}^{3+}$  and  $\text{Mn}^{4+}$  ions decreases, which leads to a decrease in the resistivity. In a magnetic field of about 15 kOe, when all the magnetic moments are aligned along the magnetic field direction (Fig. 5), the resistivity reaches its minimum value, since the angle between the spins of  $\text{Mn}^{3+}$  and  $\text{Mn}^{4+}$  ions becomes zero. The resistivity values for the saturation field configurations  $H \parallel c$  and  $H \parallel ab$  coincide (Fig. 4).

As the temperature is increased to  $T = 55 \text{ K}$ , the positive magnetoresistance effect disappears, since the resistivity starts sharply increasing at approaching the AFM ordering temperature  $T_N = 65 \text{ K}$ . Therefore, the magnetization decreases due to the enhancement of local thermal fluctuations of the magnetic moments (Fig. 2). Against the background of the thermal fluctuations, the positive magnetoresistance effect becomes negligible (Fig. 3).

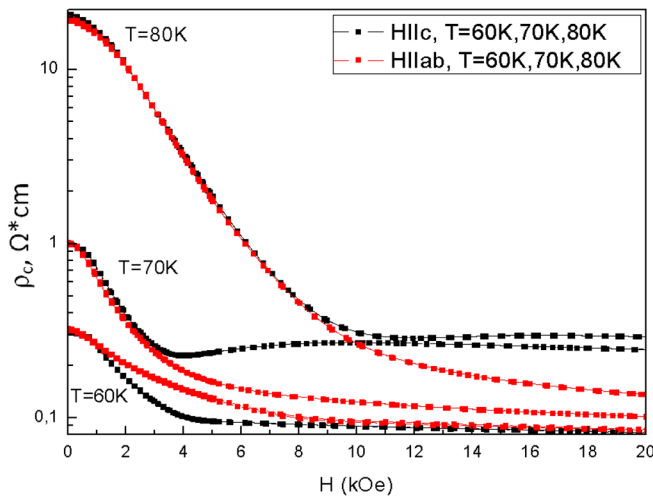


FIG. 10. Magnetic-field dependence of out-of-plane resistivity  $\rho_c$  for the  $(\text{La}_{0.9}\text{Nd}_{0.1})_{1.4}\text{Sr}_{1.6}\text{Mn}_2\text{O}_7$  single crystal at the temperatures  $T = 60, 70$ , and  $80\text{ K}$  in the field applied along the  $c$  axis and in the  $ab$  plane.

According to the literature data,<sup>21</sup> upon doping the initial composition with Nd, the crystal lattice is compressed along the  $c$  axis and the balance between the FM and AFM interactions of the bilayers shifts toward the AFM interaction. Thus, the larger part of the sample, as compared to the composition without Nd, remains in the AFM phase and the angle between the magnetic moments is larger than in the initial composition. In contrast to the initial compound, in which the easy magnetization axis is the  $c$  axis,<sup>22</sup> the FM phase of the  $(\text{La}_{0.9}\text{Nd}_{0.1})_{1.4}\text{Sr}_{1.6}\text{Mn}_2\text{O}_7$  sample has the easy magnetization plane (the  $ab$  plane). Obviously, the occurrence of the positive magnetoresistance in the sample, as in the initial compound, is related to its magnetic structure. Further investigation is needed for the shift of the positive magnetoresistance effect to the high-temperature region in an external field, for the occurrence of the effect in a field applied in the other crystallographic direction in the Nd-doped sample, as well as for the discrepancy between the saturation magnetoresistance values in the fields  $H \parallel c$  and  $H \parallel ab$  (Fig. 10).

## CONCLUSIONS

The temperature dependences of magnetoresistance of the synthesized single-crystals  $\text{La}_{1.4}\text{Sr}_{1.6}\text{Mn}_2\text{O}_7$  and  $(\text{La}_{0.9}\text{Nd}_{0.1})_{1.4}\text{Sr}_{1.6}\text{Mn}_2\text{O}_7$  samples were investigated in a wide temperature range in external magnetic fields applied

along the  $c$  axis and in the  $ab$  plane of the crystals. For the first time, the positive magnetoresistance effect was detected for these crystals. In the  $\text{La}_{1.4}\text{Sr}_{1.6}\text{Mn}_2\text{O}_7$  sample, the effect was observed in a magnetic field applied along the  $ab$  plane in the temperature range  $T = 4.2\text{--}50\text{ K}$ , while in the doped  $(\text{La}_{0.9}\text{Nd}_{0.1})_{1.4}\text{Sr}_{1.6}\text{Mn}_2\text{O}_7$  crystal, the effect occurs in a field applied in the  $c$  plane at higher temperatures (about  $T = 60\text{ K}$ ). We showed that the positive magnetoresistance originates from spin-dependent tunneling of carriers between the manganese-oxygen bilayers and can be explained by features of the magnetic structure of the investigated compounds consisting of two magnetic phases, which arise at different temperatures.

- <sup>1</sup>T. Kimura and Y. Tokura, *Annu. Rev. Mater. Sci.* **30**, 451 (2000).
- <sup>2</sup>M. B. Salamon and M. Jaime, *Rev. Mod. Phys.* **73**(3), 583 (2001).
- <sup>3</sup>C. Zener, *Phys. Rev.* **82**(3), 403 (1951).
- <sup>4</sup>A. J. Millis, P. B. Littlewood, and B. I. Shraiman, *Phys. Rev. Lett.* **74**(25), 5144 (1995).
- <sup>5</sup>A. M. Goldman, *Science* **274**(5293), 1630 (1996).
- <sup>6</sup>C. N. R. Rao, P. Ganguly, K. K. Singh, and R. A. Ram, *J. Solid State Chem.* **72**(1), 14 (1988).
- <sup>7</sup>J. B. Goodenough, *J. Appl. Phys.* **81**, 5330 (1997).
- <sup>8</sup>Y. Tokura, Y. Tomioka, H. Kuwahara, A. Asamitsu, Y. Moritomo, and M. Kasai, *J. Appl. Phys.* **79**(8), 5288–5291 (1996).
- <sup>9</sup>Y. Moritomo and A. Asamitsu *et al.*, *Nature* **380**, 141–144 (1996).
- <sup>10</sup>M. Matsukawa, M. Chiba, A. Akasaka, R. Suryanarayanan *et al.*, *Phys. Rev. B* **70**, 132402 (2004).
- <sup>11</sup>K. Dörr, K. H. Müller, L. Schultz, K. Ruck, and G. Krabbes, *J. Appl. Phys.* **87**, 814–816 (2000).
- <sup>12</sup>Y. Moritomo, *Aust. J. Phys.* **52**, 255 (1999).
- <sup>13</sup>D. N. Argyriou, J. F. Mitchell, P. D. Radaelli, H. N. Bordallo *et al.*, *Phys. Rev. B* **59**(13), 8695 (1999).
- <sup>14</sup>M. Kumaresavanji, M. S. Reis, Y. T. Xing, and M. B. Fontes, *J. Appl. Phys.* **106**(9), 093709 (2009).
- <sup>15</sup>K. Mydeen, S. Arumugam, P. Mandal, A. Murugeswari, C. Sekar, G. Krabbes, and C. Q. Jin, *J. Appl. Phys.* **106**(10), 103908 (2009).
- <sup>16</sup>H. Zhu, D. Zhu, and Y. Zhang, *J. Appl. Phys.* **92**(12), 7355–7361 (2002).
- <sup>17</sup>J. F. Mitchell, C. D. Ling, J. E. Millburn, D. N. Argyriou, A. Berger, and M. Medarde, *J. Appl. Phys.* **89**, 6618–6620 (2001).
- <sup>18</sup>H. Sonomura, T. Terai, T. Kakeshita, T. Osakabe, and K. Kakurai, *Phys. Rev. B* **87**, 184419 (2013).
- <sup>19</sup>L. Malavasi, M. Baldini, I. Zardo, M. Hanfland, and P. Postorino, *Appl. Phys. Lett.* **94**, 061907 (2009).
- <sup>20</sup>A. D. Balaev, Yu. V. Boyarshinov, M. M. Karpenko, and B. P. Khrustalev, *Instrum. Exp. Tech.* **26**(3), 167 (1985).
- <sup>21</sup>Y. Moritomo, K. Okoyama, and M. Ohashi, *Phys. Rev. B* **59**, 157 (1999).
- <sup>22</sup>A. N. Lavrov, L. P. Kozeeva, M. R. Trunin, and V. N. Zverev, *J. Supercond. Novel Magn.* **22**, 63 (2009).
- <sup>23</sup>K. A. Shaykhtudinov, S. V. Semenov, S. I. Popkov, D. A. Balaev, A. A. Bykov, A. A. Dubrovskiy, and N. V. Volkov, *J. Appl. Phys.* **109**(8), 083711 (2011).
- <sup>24</sup>W. Anderson and H. Hasagawa, *Phys. Rev.* **100**, 675 (1955).